Charge-self-consistent band structure of TiC, TiN, VC and VN

1990 J. Phys.: Condens. Matter 2 9363

(http://iopscience.iop.org/0953-8984/2/47/011)

J. Phys.: Condens. Matter 2 (1990) 9363–9371. Printed in the UK

Charge-self-consistent band structure of TiC, TiN, VC and VN

V A Pai†, A P Sathe† and V R Marathe‡

† The Institute of Science, 15 Madame Cama Road, Bombay 400 032, India

‡ Tata Institute of Fundamental Research, Homi Bhabha Road, Bombay 400 005, India

Received 12 March 1990, in final form 4 June 1990

Abstract. Charge-self-consistent LCAO band-structure calculations have been carried out for transition-metal compounds TiC, TiN, VC and VN and compared with experimental data. The effective atomic charges calculated self-consistently, employing the Mulliken population analysis, are used to study the charge transfer. The calculations have been used mainly to compare

(i) the density of states with photoelectron spectra and

(ii) the bands along Γ–X with the available angle-resolved photoelectron spectroscopy data.

In order to study the vacancy effect in these compounds, the same method was applied to a typical case of $TiC_{0.75}$. The calculations account for the trends that are observed experimentally.

1. Introduction

The band structures of the transition-metal monocarbides and mononitrides, which have a simple rock-salt structure, continue to be studied by researchers because of their interesting physical and chemical properties. They possess metallic conductivity, superconductivity, extremely high melting point, extreme hardness and brittleness. Some of the transition-metal carbides and nitrides such as NbC, TaC and MoN have superconducting temperatures above 11 K [1]. These properties are suggestive that the covalent, ionic and metallic bondings are present simultaneously. Several calculations have been carried out on TiC, TiN, VC and VN, beginning with the work of Bilz [2], who used the tight-binding method. In many of these studies, vacancy effects have been considered also as these compounds have a tendency to form non-stoichiometrically. In view of the very useful reviews [3–5] on various aspects of these compounds, we shall refer to only a few reports which we consider important here. Neckel *et al* [6] have carried out APW calculations on these compounds with the LCAO interpolation scheme. The total and partial density of states (DOS), along with a charge analysis, were presented. Much of the subsequent experimental work [7–12] has been compared with their results. Dunard *et al* [13] have estimated the charge transfer in $TiC_{0.94}$ and $TiN_{0.99}$ by means of high-precision x-ray diffraction. A sophisticated atomic model was introduced to extrapolate the results to stoichiometric composition and compared with the LAPW results of Blaha *et al* [14]. They concluded that the metal-to-metal bonding is similar in

0953-8984/90/479363 + 09 $03.50

TiC and TiN while the metal-to-non-metal bonding is greater in TiC than in TiN. The KKR CPA calculations on substoichiometric TiC_x, TiN_x, VC_x and VN_x for a wide range of x in these compounds were carried out by Marksteiner *et al* [15]. Beauprez *et al* [11] have carried out x-ray photoelectron spectroscopy (XPS) to study the vacancy effects in TiN_x ($0.35 \leqslant x \leqslant 1$) and have found good agreement with their KKR CPA calculations. The vacancy-induced electronic structure of several transition-metal carbides and nitrides, as would be observable in x-ray photoemission intensities, was calculated by Redinger *et al* [16] and compared with XPS measurements. The substoichiometric compositions of NbC_x, TaC_x and HfC_x, for $0.7 \leqslant x \leqslant 1.0$, have been studied by Klein *et al* [17] using the LCAO CPA method. Their method closely follows the tight-binding CPA method [18]. The electronic properties, including superconductivity, of several stoichiometric group-V and group-VI nitrides have been studied by Papaconstantopoulos *et al* [19]. Zukov *et al* [20] have discussed the effects of vacancy formation and the chemical binding by LMTO ASA method and analysed a large amount of experimental data in the light of their calculations. Recently, Kim *et al* [21] have reported the application of the mixed-basis band-structure interpolation scheme (MBBSIS) to study the band structure and charge densities of some of these stoichiometric compounds.

There are several experimental studies using different techniques of spectroscopy such as XPS, ultraviolet photoelectron spectroscopy (UPS) and angle-resolved photoelectron spectroscopy [22–24]. As the XPS spectrum directly reflects the main features of the DOS of the occupied states, the calculated DOS can be compared with it; the ARPES studies on single crystals enable a better comparison of the calculated bands with experiment to be made.

The methods used to calculate the band structure employ a number of approximations and assumptions. The agreement with experiment is often partial. This leaves scope for more systematic work. The charge-self-consistent band-structure (CSCBS) method of calculation, used in this work, was successfully employed earlier in the interpretation of photoelectron and optical spectra of perovskites and pyrites [25, 26]. As charge-self-consistency has been explicitly built into our calculations, we expect our calculations to be reliable.

2. Calculational aspects

2.1. Theoretical model

In the CSCBS calculations the Bloch sums are used as the basis. If $\phi_a(\boldsymbol{r} - \boldsymbol{R}_l)$ are atomic orbitals centred at positions $\boldsymbol{R}_l$, then the corresponding Bloch sum is given by

$$X_a(\boldsymbol{k}; \boldsymbol{r}) = N_a(\boldsymbol{k}) N^{-1/2} \sum_{l=1}^{N} \exp(\mathrm{i}\boldsymbol{k} \cdot \boldsymbol{R}_l)\, \phi_a(\boldsymbol{r} - \boldsymbol{R}_l) \tag{1}$$

where $N_a(\boldsymbol{k})$ is the normalisation constant and N is the number of lattice points (in reality $N \rightarrow \infty$). The wavefunctions are given by

$$\Psi_i(\boldsymbol{k}; \boldsymbol{r}) = \sum_a C_{ai}(\boldsymbol{k}) X_a(\boldsymbol{k}; \boldsymbol{r}). \tag{2}$$

The periodicity conditions are present in respect of the wavefunctions and potentials. The overlap integral between two Bloch sums is given by

$$S_{ab}(\boldsymbol{k}) = \int X_a^*(\boldsymbol{k}; \boldsymbol{r}) X_b(\boldsymbol{k}; \boldsymbol{r})\, \mathrm{d}^3\boldsymbol{r}. \tag{3}$$

Using equation (1) we get

$$S_{ab}(\boldsymbol{k}) = N_a(\boldsymbol{k})N_b(\boldsymbol{k}) \sum_l \exp(i\boldsymbol{k}\cdot\boldsymbol{R}_l) S_{ab}^{\mathrm{AO}}(\boldsymbol{R}_l) \tag{4}$$

where

$$S_{ab}^{\mathrm{AO}}(\boldsymbol{R}_l) = \int \varphi_a^*(\boldsymbol{r})\varphi_b(\boldsymbol{r}-\boldsymbol{R}_l)\,\mathrm{d}^3\boldsymbol{r} \tag{5}$$

is the atomic overlap integral between the orbitals φ_a and φ_b centred at lattice points $\mathbf{0}$ and $\boldsymbol{R}_l$, respectively. A similar procedure undertaken for the electronic Hamiltonian would give

$$H_{ab}(\boldsymbol{k}) = N_a(\boldsymbol{k})N_b(\boldsymbol{k}) \sum_l \exp(i\boldsymbol{k}\cdot\boldsymbol{R}_l) \int \varphi_a^*(\boldsymbol{r})\hat{H}\varphi_b(\boldsymbol{r}-\boldsymbol{R}_l)\,\mathrm{d}^3\boldsymbol{r}. \tag{6}$$

At this stage, a few approximations are made. As in the case of the extended Huckel MO theory, the Hamiltonian integral is written as

$$\int \varphi_a^*(\boldsymbol{r})\hat{H}\varphi_a(\boldsymbol{r})\,\mathrm{d}^3\boldsymbol{r} = h_{aa} = -(P_a^{\mathrm{I}} + P_{\mathrm{A}}^{\mathrm{M}}) \tag{7}$$

where P_a^{I} is the ionization potential of the electron in the orbital φ_a on atom A and $P_{\mathrm{A}}^{\mathrm{M}}$ is the Madelung potential at A. On the basis of Cusachs' [27] approximation, the off-diagonal matrix element is taken as

$$\varphi_a^*(\boldsymbol{r})\hat{H}\varphi_b(\boldsymbol{r}-\boldsymbol{R}_l)\,\mathrm{d}^3\boldsymbol{r} = S_{ab}^{\mathrm{AO}}(\boldsymbol{R}_l)[(1.1 - 0.6|S_{ab}^{\mathrm{AO}}(\boldsymbol{R}_l)|)(h_{aa} + h_{bb}) - (Q_{\mathrm{A}} + Q_{\mathrm{B}})/R_{\mathrm{AB}}] \tag{8}$$

where Q_{A} and Q_{B} are the effective atomic charges of the atoms A and B, respectively, which are calculated using the Mulliken population analysis [26] and R_{AB} is the distance between the atoms at A ($\mathbf{0}$) and B ($\boldsymbol{R}_l$). Using equations (7) and (8) in equation (6), we obtain the Hamiltonian matrix $H(k)$.

The Schrödinger equation, then, can be written as

$$H(\boldsymbol{k})C(\boldsymbol{k}) = S(\boldsymbol{k})C(\boldsymbol{k})E(\boldsymbol{k}). \tag{9}$$

Adopting the procedure described in [25] the diagonal matrix of energies $E(\boldsymbol{k})$ and the matrix of the coefficients $C(\boldsymbol{k})$ of the linear combination of Bloch sums are obtained for every value of $\boldsymbol{k}$. Subsequently, new effective charges are calculated using integration over the whole $\boldsymbol{k}$-space [26]. This new effective charge is utilized to calculate the new Madelung and ionization potentials. The ionization potential is calculated with respect to the new charge using the relation [26]

$$P_a^{\mathrm{I}} = P_{a0}^{\mathrm{I}} + \Delta P_a^{\mathrm{I}}\, Q_{\mathrm{A}} \tag{10}$$

where P_{a0}^{I} is the atomic valence ionization potential and ΔP_a^{I} is its incremental value. At this stage, one is back to the starting point with new P_a^{I} and $P_{\mathrm{A}}^{\mathrm{M}}$, and hence new $H_{ab}(\boldsymbol{k})$. Therefore, equation (9) can be solved iteratively until charge self-consistency is reached.

2.2. *Parametrization*

The valence ionization potentials P_{a0}^{I} were taken from atomic HF calculations [28] and their incremental values ΔP_a^{I} were parametrized. Slater-type single ζ orbitals (STOs)

Table 1. The Slater exponent ζ, the atomic valence ionization potential P^{1}_{a0} and the incremental ionization potential ΔP^{1}_{a} of the orbitals of the basis considered in the CSCBS calculations.

Atom	Orbital	ζ	P^{1}_{a0} (Hartree)	ΔP^{1}_{a} (Hartree)
C	2s	1.72	0.76563	0.47
	2p	1.72	0.43335	0.47
N	2s	1.95	1.00531	0.50
	2p	1.95	0.56758	0.50
Ti	4s	1.70	0.20513	0.43
	4p	1.70	0.07669	0.43
	3d	2.27	0.27342	0.43
V	4s	1.70	0.21441	0.43
	4p	1.70	0.08597	0.43
	3d	2.34	0.32069	0.43

were used throughout and their exponents ζ taken were the same as the scaling factors for the STO NG basis sets [29]. The atomic valence orbitals which have been used in the investigation are 4s, 4p, 3d on the transition metal and 2s, 2p on the non-metal. The values of P^{1}_{a0}, ΔP^{1}_{a} and ζ for all the four compounds are given in table 1. The Madelung potentials P^{M}_{A}, which are charge dependent, are required to be calculated in each iteration. They were calculated using a recent procedure [30] which involves a direct summation technique.

2.3. Structural data, k-space integration and density-of-states calculation

All of the stoichiometric compounds studied have a simple rock-salt structure which is a FCC Bravais lattice. The basis consists of one type of atom at (0, 0, 0) and the other type at $(a/2)$ (1, 0, 0) of the conventional cubic cell. The values of the lattice constant a in A taken in the calculations are 4.329 [14], 4.242 [6], 4.182 [6] and 4.137 [12] for TiC, TiN, VC and VN, respectively. For the stoichiometric compositions the charge-self-consistent calculations were carried out using 89 points in the irreducible wedge of the FCC FBZ, taking advantage of the symmetry. Considering the symmetry of the crystal, this is equivalent to 2048 points in the FBZ. A systematic variation in the number of $\boldsymbol{k}$-points did not show any appreciable improvement of the results with an increased number of $\boldsymbol{k}$-points beyond 2048. For the non-stoichiometric composition $TiC_{0.75}$, a simple cubic unit cell with seven atoms (one carbon missing), as described in [20], was considered. The number of $\boldsymbol{k}$-points used in the FBZ was reduced to 216 to reduce the computational time of the self-consistent calculations. The condition of convergence with respect to the charge was $0.05e$ per atom in all the cases.

The DOS is calculated using the equation

$$n(E) = \frac{\Omega}{8\pi^3} \int_{FBZ}^{\text{occupied}} \sum_i \delta[E_i(\boldsymbol{k}) - E]\, \mathrm{d}^3\boldsymbol{k} \tag{11}$$

where δ is the Dirac delta function. In the actual calculation we obtained $n(E)$ by replacing the δ function by a Gaussian:

$$\delta(E - E_i) \rightarrow [1/\sqrt{2\pi}\sigma] \exp[-(E_i - E)^2/2\sigma^2] \tag{12}$$

where σ is the half-width of the Gaussian which in the present calculations is taken to be 0.005 Hartree.

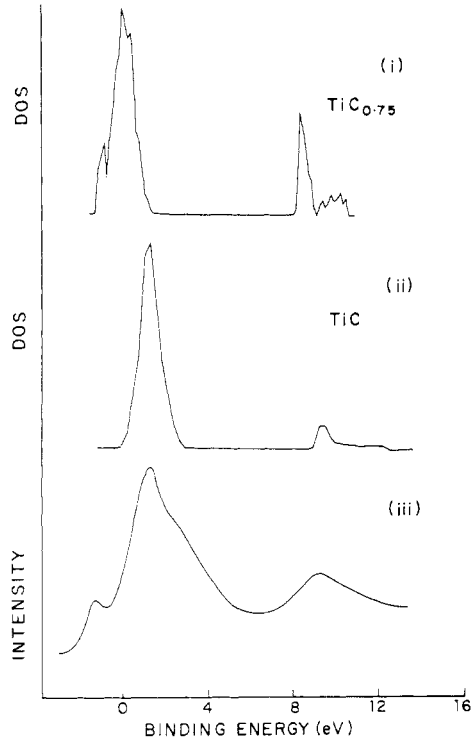

Figure 1. Comparison of the DOS of $TiC_{0.75}$ (curve (i)), the DOS of TiC (curve (ii)) and the photoelectron spectrum of TiC (curve (iii)) [7].

3. Results and discussion

With the calculational aspects outlined in section 2, we have determined the electronic structure of stoichiometric TiC, TiN, VC and VN. The vacancy effects studied by the same method have been reported only in the case of $TiC_{0.75}$ as a typical case of these compounds. The DOSs have been compared with the photoelectron spectra, and the bands in a certain direction of high symmetry in k-space have been compared with the ARPES results reported in the literature. Since, in our calculation, we are comparing the photoelectron spectra generally with band positions and not with the actual intensity profile, we have not incorporated the effects of the cross sections.

3.1. Band structure of TiC

In figure 1, curve (iii) is the photoelectron spectrum of TiC reported by Johansson *et al* [7] and curve (ii) is the DOS of stoichiometric TiC. It is found that the agreement is not good because there is an additional peak near E_F in the experimental curve. In order to study the origin of this additional peak we did calculations in $TiC_{0.75}$ assuming an ordered vacancy model. This may be a poor approximation in view of the fact that experimental carbon vacancies are not as high as 25% and are also not periodically ordered. However, in the present calculations we only wish to monitor the change in DOS due to the presence of the vacancies. The experimental photoelectron spectra then can be considered to arise from the superposition of the bulk DOS and vacancy-modified DOS. Curve (i) is the DOS of this substoichiometric composition. The zero of the energy corresponds to

Table 2. Comparison of calculated and experimental energies for some selected states for TiC. The energies are relative to the Fermi level.

State	Energy (eV)		
	Experimental [9]	CSCBS	APW [6]
Γ_1	-13 ± 0.3	-12.6	-12
L_1	-10.9 ± 0.3	-9.5	-8.6
X_1	-10.5 ± 0.3	-9.9	-10
L_2'	-6	-3.1	-5.6
L_3'	-3.6	-2.0	-2.6
X_4'	-4	-1.2	-3.2
X_3	—	-0.5	-1.7
X_5'	-0.5	-0.1	-0.1

the Fermi level of stoichiometric TiC. It is important to note that the main peaks predominantly due to carbon 2p states do not coincide in curves (i) and (ii). The Fermi level is shifted to higher energies in the presence of vacancies. There is a diffuse structure near the carbon 2s peak in curve (i). The main peak in the experimental curve has been matched with that of the stoichiometric composition. The DOS feature in curve (iii) can easily be seen to be the superposition of the DOS features seen in curves (i) and (ii). Therefore, we conclude that curve (iii) corresponds to a substoichiometric composition with a small amount of carbon vacancies. However, it is not possible to give a quantitative estimate of the concentration of vacancies responsible for these features. The KKR calculations [15] for substoichiometric TiC also showed a vacancy peak in the DOS and an increase in the Fermi energy. The CSCBS energies for some selected states of TiC are compared with the ARPES results [9] and the APW calculations [6] in table 2. Our calculations agree well with the experimental band structure as well as the APW results. The effective atomic charge of Ti and TiC is found to be $1.73e$ (an equal but negative charge on the carbon atom) which compares well with the experimental [13] value of $2.05e$.

3.2. Band structure of TiN

In figure 2, we have compared the calculated DOS of TiN with the photoelectron spectra of $TiN_{0.99}$ [24] for a photon energy of 40 eV in curve (i) and of $TiN_{0.83}$ [7] for a photon energy of 90 eV in curve (ii). The agreement with experiments, irrespective of the vacancies, is very good. In figure 3 the calculated bands and experimental bands [22] along the $\langle 1\,0\,0 \rangle$ direction for TiN are shown. It is observed that the calculated and experimental Δ_2' bands almost coincide. The calculated Δ_5 band is rather flat and is away from the Fermi level and the Δ_1 band is near to the Fermi level, compared with experiment. The calculated effective atomic charge of Ti in TiN is $1.98e$ which compares well with the experimental value of $1.91e$ [13].

3.3. Band structure of VC

As this compound does not form easily without having vacancies, there are few experimental reports available on its stoichiometric composition. In figure 4, the total DOS

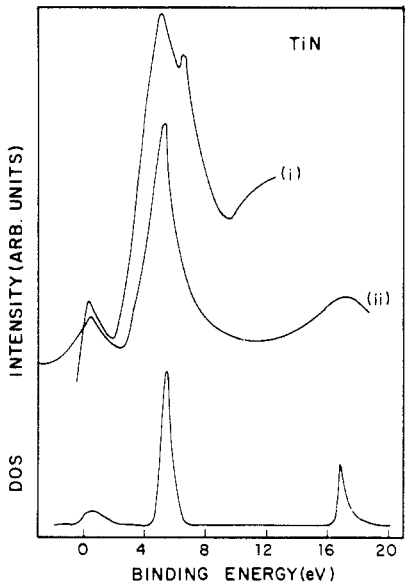

Figure 2. Comparison of the total DOS and valence band photoemission spectra [7, 24] of TiN.

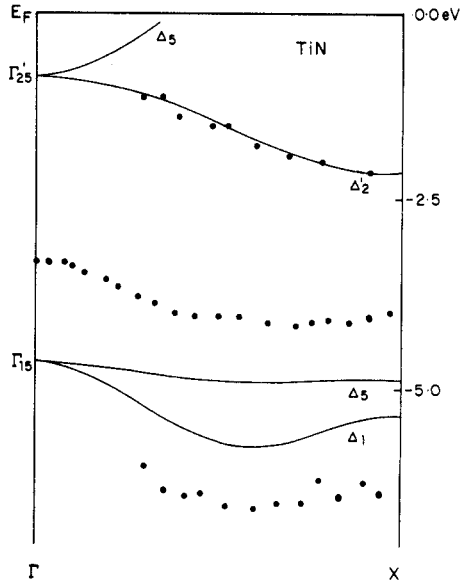

Figure 3. Comparison of calculated (——) and experimental (●) [22] energy band dispersions along the ⟨1 0 0⟩ direction for TiN.

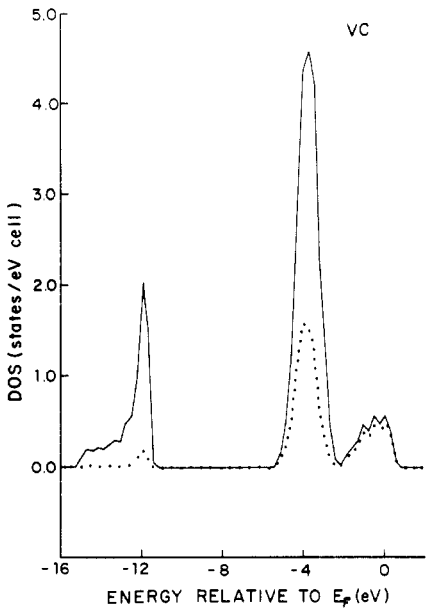

Figure 4. Calculated total DOS (——) and partial DOS (. . . . .) of 4s, 4p and 3d orbitals of V in VC.

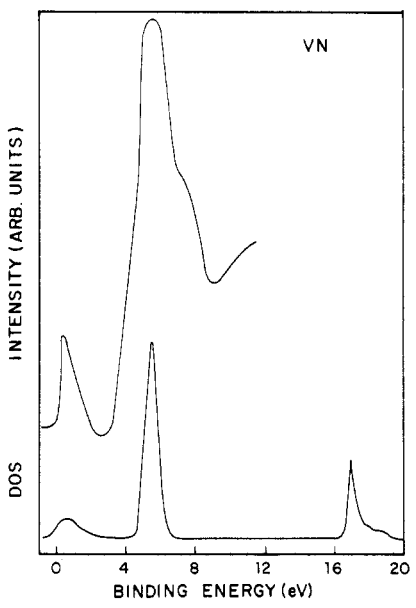

Figure 5. Comparison of DOS and valence band photoemission spectra [31] for VN.

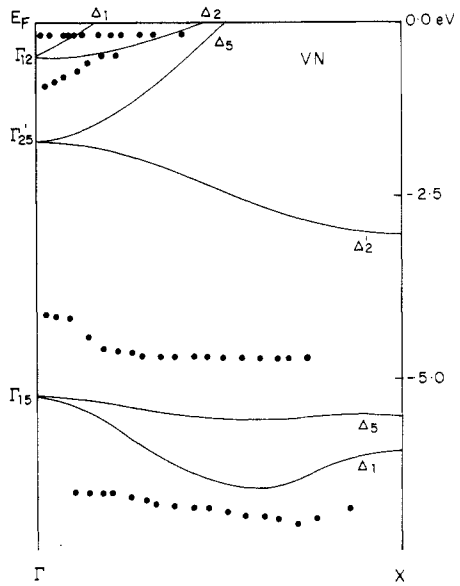

Figure 6. Comparison of calculated (——) and experimental (●) [23] energy band dispersions along the ⟨1 0 0⟩ direction for VN.

and partial DOS due to 4s, 4p and 3d orbitals of vanadium in VC are given. Fair agreement with the recent calculations reported by Zukov *et al* [20] has been found.

3.4. Band structure of VN

In figure 5 the calculated DOS of VN is compared with the photoelectron spectra [31] of nearly stoichiometric δ-VN, which has an NaCl structure, at a photon energy of 21.2 eV. The agreement between the two is good. The experimental ARPES energy bands along the ⟨1 0 0⟩ direction [23] have been compared with the calculated bands in figure 6. The calculated Δ_5 band is away from the Fermi level and the Δ_1 band is near to it, compared with the corresponding experimental bands. In the case of other bands, calculated and experimental positions relative to E_F have similar trends as observed by Lindstrom *et al* [23]. The calculated effective atomic charge of V in VN is 2.0*e* which is rather large compared with the experimental value of 1.2*e* [12].

4. Conclusions

The CSCBS calculations were carried out for stoichiometric transition-metal monocarbides and mononitrides: TiC, TiN, VC and VN. The results explain the charge-transfer, DOS and energy band dispersion and compare well with the experimental data reported in the literature. The vacancy effects in these compounds were studied by applying the same method to $TiC_{0.75}$, as a typical case assuming an ordered vacancy model and some of the experimental observations have been explained with the help of our results.

Acknowledgments

One of the authors (VAP) wants to thank The University Grants Commission, Government of India, for the teacher-fellowship, F.2-63/86(B-2), awarded to him. A part of this work was carried out during the tenure of the fellowship.

References

[1] Vandenberg J M and Matthias B T 1974 *Mater. Res. Bull.* **9** 1085
[2] Bilz H 1958 *Z. Phys.* **153** 338
[3] Calais J-L 1977 *Adv. Phys.* **26** 847
[4] Neckel A 1983 *Int. J. Chem.* **33** 1317
[5] Zukov V P, Medvedeva N I and Gubanov V A 1989 *Phys. Status Solidi* b **151** 407
[6] Neckel A, Rastl P, Eibler R, Weinberger P and Schwarz K 1976 *J. Phys. C: Solid State Phys.* **9** 579
[7] Johansson L I, Stefan P M, Shek M L and Christensen A N 1980 *Phys. Rev.* B **22** 1032
[8] Weaver J H and Schmidt F A 1980 *Phys. Lett.* **77A** 73
[9] Weaver J H, Bradshaw A M, Vander Veen J F, Himsel F J, Eastman D E and Politis C 1980 *Phys. Rev.* B **22** 4921
[10] Höchst H, Bringans R D, Steiner P and Wolf Th 1982 *Phys. Rev.* B **25** 7183
[11] Beauprez E, Hague C F, Mariot J M, Teyssandier F, Redinger J R, Marksteiner P and Weinberger P 1986 *Phys. Rev.* B **34** 886
[12] Kubel F, Flack H D and Yvon K 1987 *Phys. Rev.* B **36** 1415
[13] Dunard A, Flack H D and Yvon K 1985 *Phys. Rev.* B **31** 2299
[14] Blaha P, Redinger J and Schwarz K 1985 *Phys. Rev.* B **31** 2316
[15] Marksteiner P, Weinberger P, Neckel A, Zeller R and Dederichs P H 1986 *Phys. Rev.* B **33** 812
[16] Redinger J, Marksteiner P and Weinberger P 1986 *Z. Phys.* B **63** 321
[17] Klein B M, Papaconstantopoulos D A and Boyer L L 1980 *Phys. Rev.* B **22** 1946
[18] Faulkner J C 1976 *Phys. Rev.* B **13** 2391
[19] Papaconstantopoulos D A, Pickett W E, Klein B M and Boyer L L 1985 *Phys. Rev.* B **31** 752
[20] Zukov V P, Gubanov V A, Jepsen O, Christensen N E and Andersen O K 1988 *J. Phys. Chem. Solids* **49** 841
[21] Kim S and Williams S 1988 *J. Phys. Chem. Solids* **49** 1307
[22] Johansson L I, Callenas A, Stefan P M, Christensen A N and Schwarz K 1981 *Phys. Rev.* B **24** 1883
[23] Lindstrom J, Lindberg P A P, Johansson L I, Law D S L and Christensen A N 1987 *Phys. Rev.* B **36** 9514
[24] Bringans R D and Hochst H 1984 *Phys. Rev.* B **30** 5416
[25] Marathe V R, Lauer S and Trautwein A X 1980 *Phys. Status Solidi* b **100** 149
[26] Lauer S, Trautwein A X and Harris F E 1984 *Phys. Rev.* B **29** 6774
[27] Cusachs J C 1965 *J. Chem. Phys.* **13** S157
[28] Clementi E and Roetti C 1974 *At. Data Nucl. Data Tables* **14** 177
[29] Hehre W J, Radom L, Schleyer P v R and Pople J A 1986 *Ab-initio Molecular Orbital Theory* (New York: Wiley) p 70
[30] Marathe V R, Lauer S and Trautwein A X 1983 *Phys. Rev.* B **27** 5162
[31] Schubert W K, Shelton R N and Wolf E I 1981 *Phys. Rev.* B **23** 5097